Natural Fracture Networks Enhancing Unconventional Reservoirs' Producibility: Mapping & Predicting*

H. Abul Khair[1], D. Cooke[1], and M. Hand [2]

Search and Discovery Article #41182 (2013)
Posted August 19, 2013

*Adapted from extended abstract prepared in conjunction with oral presentation at AAPG Annual Convention and Exhibition, Pittsburgh, Pennsylvania, May 19-22, 2013

[1]Australian School of Petroleum, University of Adelaide, North Terrace, Adelaide, Australia (hani.abulkair@adelaide.edu.au)
[2]SA Centre for Geothermal Energy Research, University of Adelaide, Australia.

Abstract

The success of an unconventional reservoir can be dependent on the density and orientation of the pre-existing natural fracture networks. We mapped and predicted natural fractures using 3D seismic data and geomechanical simulation for tight gas reservoirs in the Cooper Basin/South Australia and compared these resulting fractures to image logs, seismic data, and well data.

We extracted positive curvature attribute in a workflow that included applying structural smoothing on the seismic cube to eliminate acquisition artifacts, then excluding low curvature values that do not reflect any structural feature. A validation procedure was applied using image logs, well data, and quality seismic, and a high correlation was found between the curvature and fractures as seen on image logs.

Another technique used integrated geological and geophysical data extracted from fault and horizon seismic interpretation with geomechanical analyses of stress, strain, and displacements associated with the structural development of the basin. Two different methods of structural reconstruction were used to predict natural fractures: The finite element method (FEM) and elastic dislocation combined with the boundary element method (BEM). The FEM method takes into account basin evolution, horizon geometry, heterogeneous rock properties, and stresses. The BEM method considers the effect of fault displacement on generating stress and strain at every node of the dislocated elastic horizon around the fault. BEM succeeds in simulating strain distribution especially close to main faults, but it does not consider rock heterogeneity or the effect of intra-seismic relaxation on fracture generation. The BEM method used here does not take into account far field stress data, which is probably why it is not possible to predict fracture networks away from the major faults.

Predicted fractures were compared to image logs. The FEM fracture prediction gives a better match to the image logs while the BEM fracture prediction fails to predict any fractures except near major faults. The BEM predictions near faults have good correlation with image logs. Our conclusion is that FEM and the enhanced most positive curvature seismic attribute can be used to model subsurface fracture networks with a high degree of accuracy.

Introduction

Well bore and completion design for unconventional reservoirs can be optimised if one has knowledge of the current day in-situ stresses, ancient stresses, and pre-existing natural fractures. One method used in this study is to use seismic attributes for estimation of pre-existing fractures. Although seismic resolution is insufficient to image fractures, the structural features mapped with seismic can be used to predict small-scale features like fractures.

Rocks may have been subjected to a large diversity of stress magnitudes and orientations during tectonic history which might have caused rock failure and generated fractures. Part of these stresses might have been stored in the rock masses and can influence the location of production sweet spots (Angelier, 1994). Another method used in this study is stress inversion for modelling of fracture networks (Gapais et al., 2000; Lisle et al., 2001; Orife and Lisle, 2003). The methodology utilizes fault slips calculated from interpreted faults and horizons in 3D seismic to restore the initial state of the rock body with the consideration of geomechanical properties, then forward modelling and calculation of the paleostresses resulted from various seismic event. Spatial distribution of these stresses is going to be examined for possible locations of generated fractures.

We conducted our study on the Moomba-Big Lake field in Cooper Basin / South Australia, which is the most recent target by the industry for unconventional reservoirs (Figure 1). Cooper Basin is a Late Carboniferous to Middle Triassic basin filled mostly with fluvial clastic sediments (Paten, 1969; Stuart, 1979; Thornton, 1979; Powell and Veevers, 1987). From the Cooper sequence, the Roseneath-Epsilon-Murteree (REM) section proved to contain significant amount of gas in the Nappamerri trough (Elliott et al., 2010).

Curvature Attributes

Seismic attributes are often used and sometimes abused in predicting fracture networks. In order to avoid attribute abuse, we use image logs and wireline logs to validate fractures predicted from seismic attributes. The most frequently used seismic attributes for predicting faults and fractures are coherence and curvature, which have been discussed by a number of authors (e.g., Hunt et al., 2010; Hakami et al., 2004; Chopra and Marfurt, 2007; Backé et al., 2011; Abul Khair et al., 2012). We found that structurally smoothed, non-steered and dip-steered, median-filtered curvature attributes, including most-positive curvature (MPC) and most negative (MNC), proved most successful in delineating folds, faults, and/or fractures (Figure 2).

Curvature is defined as the reciprocal of the radius of a circle that is tangent to the given curve at a point (Chopra and Marfurt, 2007). An observed high value of curvature corresponds to curve; whereas curvature will be zero for a straight line (the same concept is applicable to surfaces). Using the curvature attribute enables mapping of geological structures, such as folds or faults, which are characterized by high curvature (Backe et al., 2011; Abul Khair et al., 2012). MPC attribute delineates up-thrown fault blocks and crests of antiforms, whilst MNC attributes delineate the down-thrown faulted blocks of faults in addition to synforms (Chopra and Marfurt, 2007). Published examples of

curvature often lack well control for validation, but this study had access to approximately 300 wells including seven image logs.

Using the background steering algorithm available through the commercial code OpendTect and Petrel, a median-filtered dip-steered cube was created. The dip-steering cube stores the maximum dip inline and crossline direction in a seismic cube. It allows highlighting of the continuity of seismic events spatially, and thus improves the accuracy of positioning of horizons, sedimentary features, and/or structural objects. Several curvature attributes were calculated using the original volume and the dip-steering cube following the method of Al-Dossary and Marfurt (2006).The most positive and most negative curvature attributes permitted the delineation of subtle structural features, which are interpreted as faults and fracture networks with variable apertures (Figure 2). To define their trend and spacing and assess the reliability of using these complex curvature attributes for the definition of natural fractures, these structures were carefully mapped and validated using image-log interpreted fractures, seismic interpreted structures, and well data.

Image Logs

A total of seven wells containing image logs were analysed and compared with the curvature signatures. More than 70% of the fractures interpreted using image logs were found to be either parallel or perpendicular to curvature signatures. By comparing the structures on seismic to the curvature signatures, antiforms were mapped as high curvature signatures reflecting the fold hinge, whereas the fractures on image logs for the same area were mostly perpendicular to that signature, with few parallel to it (Figure 3).

The relation between the image log fractures and curvature signatures can be interpreted in many ways. During the formation of an anticline, the maximum horizontal stress (SHmax) is perpendicular to the fold axis; this will cause fracture initiation and propagation in the direction of SHmax if the rock reached failure conditions according to its elastic properties, and if the differential stress was high. Due to the maximum bending at the hinge of the anticline, high strain along the hinge of the fold will cause weakness of the rocks and a new set of fractures is expected to open parallel to the hinge and perpendicular to the old set. If we added to this scenario the existence of an old set of fractures that was generated due to an older tectonic event in a direction that might be different than the event that caused folding, then we will have a group of fracture sets, as in Figure 4, that are not supposed to have consistent correlation with the current structures, and so with the curvature signature. Thus, curvature attributes will map indirectly fractures caused by the formation of the current fold and faults.

Seismic Amplitudes

By comparing the curvature signatures to the seismic structures, a high correlation was found with most of the curvature signatures presented on seismic sections as either antiforms or small faults with offsets 1 ms or more. A new seismic volume was generated using all the curvature signatures (more than a cut-off value) that represent seismic artifacts and do not map any structure. This value should be examined for every survey by comparing the curvature values to seismic structures before generating the new volume that represents only the available structures (Figure 5)

Well Control

Considering the fact that any fault cutting a well will cause a variation in the thickness of the crossed formation depending on the fault type, a survey was conducted by calculating the thickness of intervals within the Roseneath Shale Formation in the Moomba-Big Lake area and compared to seismic and curvature signatures. A consistent relationship was found between the increase and decrease of the thickness with the seismic and curvature signatures. It was found that whenever a thickness change exists, a deep fault will be seen on seismic, although it might not be cutting the target horizon at shallower depths. This indicates that the fault exists, but seismic resolution cannnot map these small offsets.

Fracture Prediction Using Stress Inversion

Over the past century, structural geologists have invested considerable effort in relating stress and fault slip to tectonic history (Price, 1966; Mandle, 1988). They used both forward and inverse modelling to solve these relationships. In forward modelling the tectonic stresses are assumed to be homogeneous and described as boundary conditions acting at some distance from the faulted rock (Hafner, 1951; Couples, 1977; Maerten et al., 1999). In inverse modelling the stress tensor is deduced from the existing geological structure plus an interpretation of fault slip, as in Carey and Burnier (1974) and Kaven et al (2011).

The method of stress inversion was first introduced by Wallace (1951) and Bott (1959), who assumed that the remote stress tensor is spatially uniform for the faulted rock and constant during the fault history, and the slip along any fault is in the same direction and sense of the maximum shear stress. These assumptions generated encouraging results and cleared the way for further usage and improvement of the technique (Pollard et al., 1993). By knowing fault orientation and slip, inversion methods are able to estimate paleostresses that caused these movements, and to predict the most likely generated structures assuming some user-supplied rock properties. These methods are the foundation for the numerous computer models that predict paleo-stresses and the resulting faults and fractures.

3D restoration and stress-strain-displacement calculation using stress inversion and forward modelling are becoming more common for unravelling geological history. This technology can also be used for validating both seismic interpretation and the main direction of deformation. Several codes are available for restoring and forward modelling geological structures, each with different input parameters and different solvers. Two common solvers used in the restoration procedure are the FEM and the BEM. The application of each methodology in the current study is discussed in detail in the following.

Dynel3D (Finite Element Method (FEM))

FEM is a numerical method for problem solving that has a big advantage over the BEM in that it can describe quite complex distributions of rock properties. In FEM, the whole object is discretised, and each element will have a simpler approximation of the solution which will be joined later with other elements of the same object to form the global solution (Hughes, 1987).

In the current study, we used a code called *Dynel3D* which utilizes geomechanics in restoring geological structures considering the physical laws (including conservation of momentum, mass, and energy) and using the linear elastic theory. Stresses that undergo permanent deformation are not considered in this code. Each element is assigned material properties which might differ laterally and vertically from other elements. If deformation exists, the code uses a solver that allows forces to be transmitted from node to node until equilibrium is obtained (Maerten and Maerten, 2006).

Dynel3D's methodology calculates stresses at the time of faulting and folding, using input seismic structural interpretation and rock properties. The estimated stresses plus user-supplied rock failure criteria are used to predict fractures. *Dynel3D* models the behaviour of folded, fractured, and faulted heterogeneous, anisotropic, and discontinuous mediums (Maerten and Maerten, 2006). Within this code, the structural model is discretised with 3D tetrahedral elements which form the mesh of the studied structure. *Dynel3D* assumes linear elasticity for structural restoration. This assumption is a potential pitfall, but it allows for a simpler and faster solution. Advantages of *Dynel3D* include the ability to model heterogeneous rock mechanical properties, ability to use friction in modelling faults, and applicability to any stress regime (Maerten and Maerten, 2006).

We applied the geomechanical restoration technique using the FEM solver in *Dynel3D* for the Moomba-Big Lake structural model. The software calculates the stress, strain, displacement, and effective stress on every node of the mesh elements within the input target horizons (Figure 6). Rock elastic properties were assigned to the shale and sandstone horizons within the Cooper Basin sequence as listed in Table 1. Restoration for every horizon was conducted to the altitude of the highest point within the same horizon. No sliding was allowed between the horizons, and they were constrained within the model boundary. Sliding was assigned for the faults without preferable direction.

The Dynel3D results (Figure 6, A and B) show a low minimum horizontal paleo-stress area along the middle of the Big Lake fault. Both the Patchawarra and Toolachee gas reservoirs have this low stress sweet spot. The Poly3D model discussed above also predicts current-day low stress in the same general area. The publicly available gas production database shows that the best producing well in Big Lake field is in this low stress area, but that same database also shows low-rate wells nearby. Our on-going research includes a more detailed study of the correlation between stress and production rate within the study area. More statistically significant results are not yet available.

Dynel3D calculates stress at each time step (during the tectonic history) and retains the highest stress experienced. The highest stresses in this model also occurred along the Big Lake Fault, presumably immediately before fault slip occurred. We compared those maximum paleo-stresses to fractures interpreted in image logs and found a correlation between maximum paleo-stress and observed fracture orientation and fracture density (Figure 7).

Traptester **(Boundary Element Method (BEM))**

The methodology, advantages, and disadvantages of using BEM as a numerical solver were discussed earlier when *Poly3D* application was introduced. We used another geomechanical restoration method through a software called *Traptester*, which is a continuum code based on

BEM (Sauter and Schwab, 2011). The methodology of the code depends on using fault slip and orientation to predict the likely distribution of subsurface strain during past tectonic events, and to predict the intensity and nature of brittle deformation (e.g., Bourne and Willemse, 2001; Bourne et al., 2001). It assumes that the main control on fracture generation is the strain perturbation around large-scale faults.

In *Traptester*, faults are represented as dislocations embedded in an isotropic elastic medium (Elastic Dislocation ED) (Crouch and Starfield, 1983). This software determines the control of large faults on the spatial and quantitative distribution of stress and strain within the rock volumes surrounding these faults (Dee et al., 2007). It models the stress and strain changes associated with elastic coseismic slip on large faults observed on seismic reflection data and neglects the effect of interseismic relaxation process. Lateral variation of rock mechanical properties are not taken into consideration when calculating the strain released during dislocation events, as it considers the structural configuration of the major faults as the dominant controller on the strain generation. Also, it uses the elastic rheology for solving the rock behaviour and strain calculation similar to the other methods.

In this study, we used the fault displacements observed on seismic reflection data as the primary input data, after running quality control studies on the interpretation to assure accurate results. Faults were then discretised into rectangular panels with horizontal upper and lower edges and uniform slip. Reduced dimensions of the panels were used with a length of 50m for better representing complex fault geometries; then displacements were calculated at each panel. Elastic strains were then computed at every point in the surrounding horizons by summing the responses to the displacements from every panel of the fault using the ED formulation of Okada (1985, 1992) and using Hooke`s law. The formulation expresses the calculated displacements according to strike, dip, dimensions, and slip vector of the faults and according to Young`s modulus and Poisson's ratio of the elastic medium, which were chosen to be 20000MPa and 0.25, respectively. Materials total density was chosen as 2000kg/m3, cohesive strength as 20MPa, and coefficient of internal friction as 0.6.

A depth correction of 2850m was applied to the calculations in order to reduce them to the appropriate syn-faulting values, as the fault network is now deeply buried compared with depths when the faults were active. No remote strains were applied to the model, as it is going to be assumed without strong base and will affect the results. The effective overburden stress was added to the redistributed stress by incorporating pore pressure of 0.01MPa/km when calculating the total stress at each point. The computed state of stress at every point was then compared to the standard Mohr-Coulomb failure envelope, using 0.75 as the fault coefficient of internal strength, and 5.5MPa as the fault cohesive material strength.

Fracturing will occur if the failure envelope is exceeded with a tensile or shear mode depending on which part of the failure envelope is exceeded first by the fault-induced calculated stresses. The angle of the failure planes relative to the principal stress axes was calculated using the standard Coulumb failure criterion (Jaeger and Cook, 1979), if shear failure is predicted. If tensile fractures are predicted, they will be oriented perpendicular to the maximum horizontal stress.

We applied the geomechanical restoration technique using *Traptester* for the Moomba-Big Lake structural model considering forward modelling in a half-space elastic medium (Figure 8). Several attributes can be calculated on the forward modelled horizons including stress,

strain, dislocation, fractures, and differential stress. As the minimum horizontal stress is used as an indicator on the location of the sweet spots, the same horizons were chosen as observation grids to display the attribute for the purpose of comparison. The same productive area in the Big Lake field show broad distinctive low stress values indicating high preference for hydraulic fracturing. However, the area addressed with the ED method is broader than the previous methods. Comparing shear and tensile fractures predicted in this method with fractures interpreted from image logs show high correlation in the wells close to Big Lake fault and low correlation away from the fault.

Summary and Conclusions

Application of the most positive curvature attribute to unconventional reservoirs leads to mapping structural features such as folds, faults, and, indirectly, fractures. Although curvature attribute calculation using normal methodology in 3D seismic causes some artifacts that confuse interpretation, the new workflow proved its validity for mapping fractures but with caution. As the curvature attributes map folds and faults, it was found that identified curvature values reflecting faults are mostly parallel to the seismic interpreted faults, and thus image-log fractures might be interpreted as fractures within the damage zones of these faults. Whereas, if the curvature attribute is mapping antiforms or synforms, the image-log fractures were found to be mainly perpendicular to the curvature signature, a relationship that indicates the current fractures present on image logs might have formed due to the stresses that caused folding. Image-log fractures parallel to folds might be interpreted as fractures formed along the hinge lines due to high strain. Accordingly, the results indicate that curvature signatures can be used to map faults, and, indirectly, fractures that are below the seismic resolution.

We have compared several methods for predicting fracture networks using stress inversion. Below are listed some major limitations of the models:

1. The geomechanical restoration methods used here assume linear, recoverable stress-strain relations, but laboratory observations show that rocks can have non-linear, non-recoverable behaviour.
2. One of the software packages exhibited an unrealistic sensitivity to changes in the input rock properties. This sensitivity leads us to question the reliability of that one package.
3. All of the software packages require the user to supply rock properties that are rarely known with accuracy.
4. Generation of fractures may be influenced by other factors that are not included in any of these models, such as paleo-temperature, bed thickness, interseismic relaxation, and stress diffusion.
5. Lateral heterogeneity in rock elastic properties has not yet been implemented in any of the software packages we used.

We used *Dynel3D* (FEM) for geomechanical restoration and estimating stresses and strains exerted during past fault movements. The low-stress locations predicted by *Dynel3D* largely match those low-stress locations predicted by Poly3D. *Dynell3D* also predicted natural fractures, and a fair correlation was found between those predicted fractures and fractures interpreted on image logs.

Traptester (BEM) also estimates natural fractures generated from past fault movements, but with the elastic dislocation method (ED). Fractures predicted by the ED method show a good correlation with image logs, but only near major faults. The ED method did not predict any fractures

away from major faults – but image logs did show fractures away from faults.

These two software packages predicted a significant low-stress area adjacent to a bend in the Big Lake Fault. The most productive well in the Big Lake Field is in this low-stress area, but so are some average performing wells. We speculate that low stress could lead to higher matrix permeability and/or more successful fracture stimulation treatments. Our ongoing work is focused on exploring the statistical correlations between gas production rate and the predicted stress and fracture density from the above models.

One of our ongoing questions is: which is more useful for development of a gas field, paleo-stress or present day stress? In our study area, paleo-stress and current day stress are very similar; so it is difficult to say which is more important or useful. However, the fractures predicted by *Dynel3D* (via structural reconstruction and paleo-stress from FEM) agree best with the fractures interpreted on image logs.

Selected References

Abul Khair, H., G. Backe, R. King, S. Holford, M. Tingay, D. Cooke, and M. Hand, 2012, Factors influencing fractures networks within permian shale intervals in the cooper basin, south Australia: APPEA Journal, v. 52, p. 213-228.

Al-Dosary, S., and K.J. Marfurt, 2006, 3-D volumetric multi-spectral estimates of reflector curvature and rotation: Geophysics, v. 17/5, p. 41-5.

Angelier, J., 1994, Fault slip analysis and palaeostress reconstruction, *in* P.L. Hancock, (ed.), Continental Deformation: Pergamon Press, Oxford, p. 53-100.

Backé G., H. Abul Khair, R. King, and S. Holford, 2011, Fracture mapping and modelling in shale-gas target in the Cooper basin, South Australia: APPEA Journal, v. 51, p. 397-410.

Bott, M., 1959, The mechanics of oblique slip faulting: Geological Magazine, v. 96, p. 109-117.

Bourne, S.J., L. Rijkels, B.J. Stephenson, and E.J.M. Willemse, 2001, Predictive modelling of naturally fractured reservoirs using geomechanics and flow simulation: GeoArabia, v. 6, p. 27-42.

Bourne, S.J., and E.J.M. Willemse, 2001, Elastic stress control on the pattern of tensile fracturing around a small fault network at Nash Point, UK: Journal of Structural Geology, v. 23, p. 1753-1770.

Carey, E., and B. Burnier, 1974, Theoretical and numerical analysis of a `basic mechanical model applied to study` al `a population failes: Proceedings of the French Academy of Sciences, Paris, Ser. D, v. 279, p. 891-894.

Chopra, S., and K. Marfurt, 2007, Volumetric Curvature Attributes adding value to 3D seismic data interpretation: The Leading Edge, v. 26, p. 856-867.

Couples, G., 1977, Stress and shear fracture (fault) patterns resulting from a suite of complicated boundary conditions with applications to the Wind River Mountains: Pure and Applied Geophysics, v. 115, p. 113-133.

Crouch, S.L., and A.M. Starfield, 1983, Boundary Element Methods in Solid Mechanics: with Applications in Rock Mechanics and Geological Engineering: Allen and Unwin, London, 322 p.

Dee, S., G. Yielding, B. Freeman, D. Healy, N. Kusznir, N. Grant, and P. Ellis, 2007, Elastic dislocation modelling for prediction of small-scale fault and fracture network characteristics: Geological Society, London, Special publications, v. 270, p. 139-155.

Gapais, D., P.R. Cobbold, O. Bourgeois, D. Rouby, and M. de Urreiztieta, 2000. Tectonic significance of fault-slip data: Journal of Structural Geology, v. 22, p. 881-888.

Hafner, W., 1951, Stress distribution and faulting: GSA Bulletin, v. 62, p. 373-398.

Hakami, A., K. Marfurt, and S. Al-Dossary, 2004, Curvature attribute and seismic interpretation: Case study from Fort Worth Basin, Texas, USA: SEG Expanded Abstracts, v. 23, p. 544.

Heidbach, O., M.R.P. Tingay, A. Barth, J. Reinecker, D. Kurfeβ, and B. Müller, 2010, Global crustal stress pattern based on the 2008 World Stress Map database release: Tectonophysics, v. 482, p. 3-15.

Hillis, R.R., and S.D. Reynolds, 2000, The Australian stress map: Journal of the Geological Society of London, v. 157, p. 915-921.

Hughes, T.J.R., 1987, The finite element method: Linear static and dynamic finite element analysis: New Jersey, Prentice-Hall, 803 p.

Hunt, L., S. Reynolds, T. Brown, S. Hadley, H. James, J. Downton, and C. Chopra, 2010, Quantitative estimate of fracture density variations in the Nordegg with azimuthal AVO and curvature: a case study: The Leading Edge, v. 29, p. 1122–1137.

Jaeger, J.C., and N.G.W. Cook, 1979, Fundamentals of Rock mechanics, 2nd Ed.: New York, Chapman and Hall, 593 p.

Kaven, J.O., F. Maerten, and D.D. Pollard, 2011, Mechanical analysis of fault slip data: Implications for paleostress analysis: Journal of Structural Geology, v. 33, p. 78-91.

Lisle, R.J., T. Orife, and L. Arlegui, 2001, A stress inversion method requiring only fault slip sense: Journal of Geophysical Research, v. 106/B2, p. 2281-2289.

Maerten, L., and F. Maerten, 2006, Chronologic modeling of faulted and fractured reservoirs using geomechanically based restoration: Technique and industry applications: AAPG Bulletin, v. 90/8, p. 1201-1226.

Maerten, L., E. Willemse, D. Pollard, and K. Rawnsley, 1999, Slip distributions on intersecting normal faults: Journal of Structural Geology, v. 21, p. 259-271.

Mandl, G., 1988, Mechanics of Tectonic Faulting. Models and Basic Concepts: Elsevier, Amsterdam, 407 p.

Okada, Y., 1985, Surface deformation due to shear and tensile faults in a half-space: Bulletin of the Seismological Society of America, v. 75, p. 1135-1154.

Okada, Y., 1992, Internal deformation due to shear and tensile faults in a half-space: Bulletin of the Seismological Society of America, v. 82, p. 1018-1040.

Orife, T., and R.J. Lisle, 2003, Numerical processing of palaeostress results: Journal of Structural Geology, v. 25, p. 949-957.

Paten, R.J., 1969, Palynologic contributions to petroleum exploration in the Permian formations of the Cooper Basin, Australia: APEA Journal, v. 9/2, p. 79-87.

Pollard, D., S. Saltzer, and A. Rubin, 1993, Stress inversion methods: are they based on faulty assumptions?: Journal of Structural Geology, v. 15, p. 1045-1054.

Powell, C.M., and J.J. Veevers, 1987, Namurian uplift in Australia and South America triggered the main Gondwanan glaciation: Nature, v. 326, p. 177-179.

Price, N.J., 1966, Fault and Joint Development in Brittle and Semi-brittle Rock: Pergamon Press, London, 176 p.

Sauter, S., and C. Schwab, 2011, Boundary elements method: Springer Series in computational mathmetics, v. 39, p. 562.

Stuart, W.J., 1976, The genesis of Permian and lower Triassic reservoir sandstones during phases of southern Cooper Basin development: APEA Journal, v. 16, p. 37-47.

Thornton, R.C.N., 1979, Regional stratigraphic analysis of the Gidgealpa Group, southern Cooper Basin, Australia: Bulletin, Gological Survey of South Australia, p. 49.

Wallace, R., 1951, Geometry of shearing stress and relation to faulting: Journal of Geology, v. 59, p. 118-130.

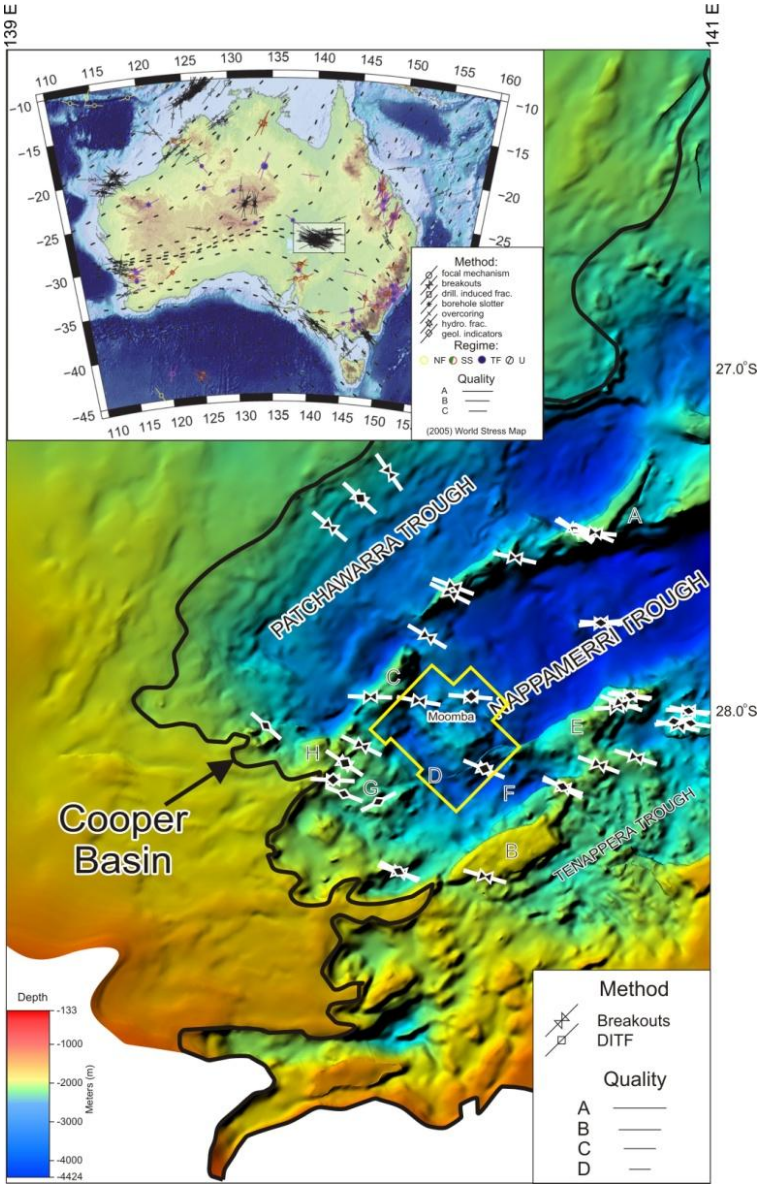

Figure 1. Top Warburton Basin (pre-Permian Basement, seismic horizon Z) in the Cooper Basin. Map shows NE-SW major troughs separated by ridges. Study area is located at the southwestern termination of the Nappamerri trough (Moomba-Big Lake 3D seismic cube outlined in yellow). A: Innamincka Ridge; B: Murteree Ridge; C: Gidgealpa-Merrimelia Ridge; Wooloo Trough; E:Della-Nappacoongee Ridge; F: Allunga Trough; H: Warra Ridge. Top left: Australian stress map (modified after Hillis and Reynolds, 2000, and World Stress Map, 2010).

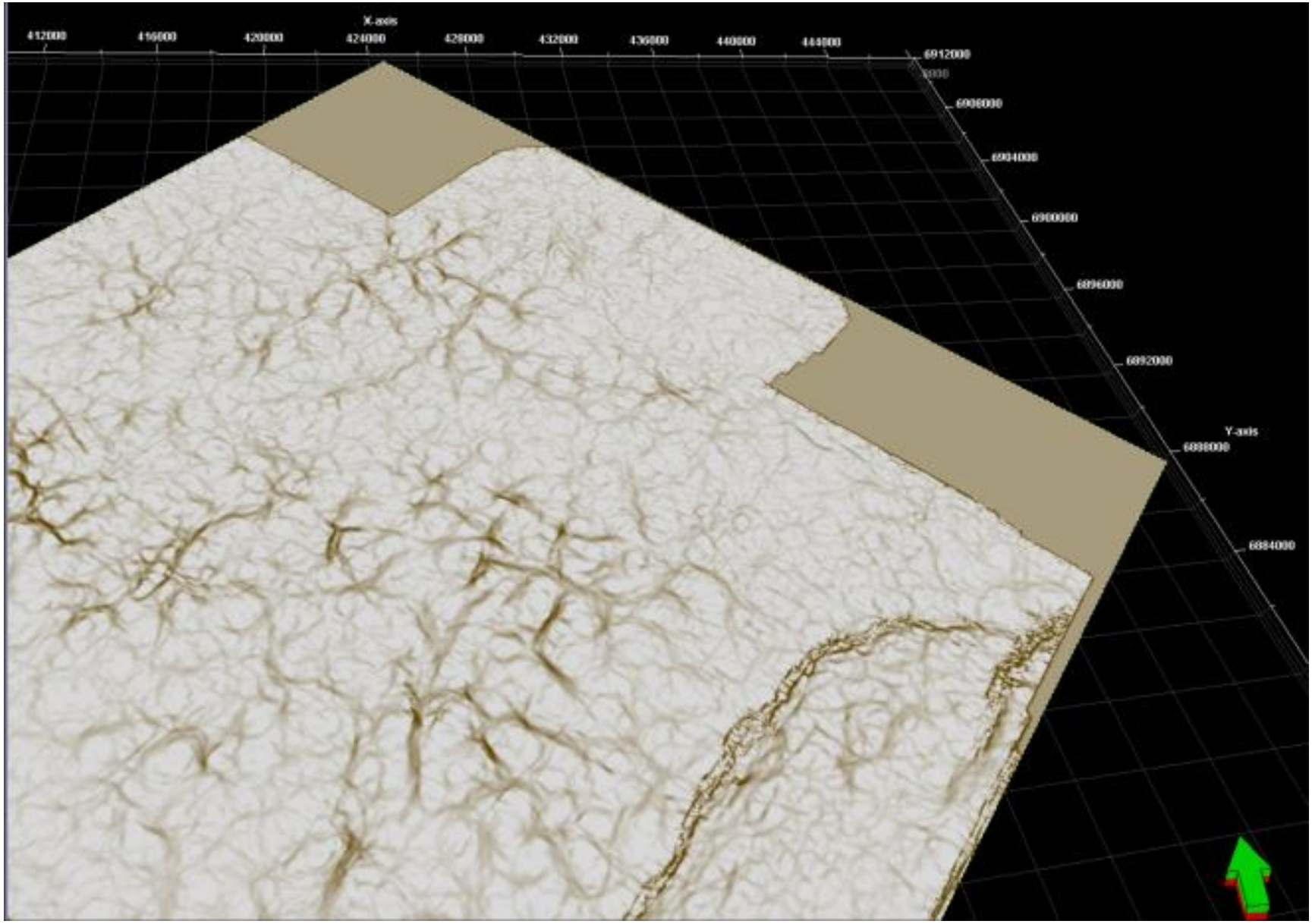

Figure 2. Most positive curvature attribute of the Moomba-Big Lake fields. Features represent faults, accompanying large fractures, and anticlines.

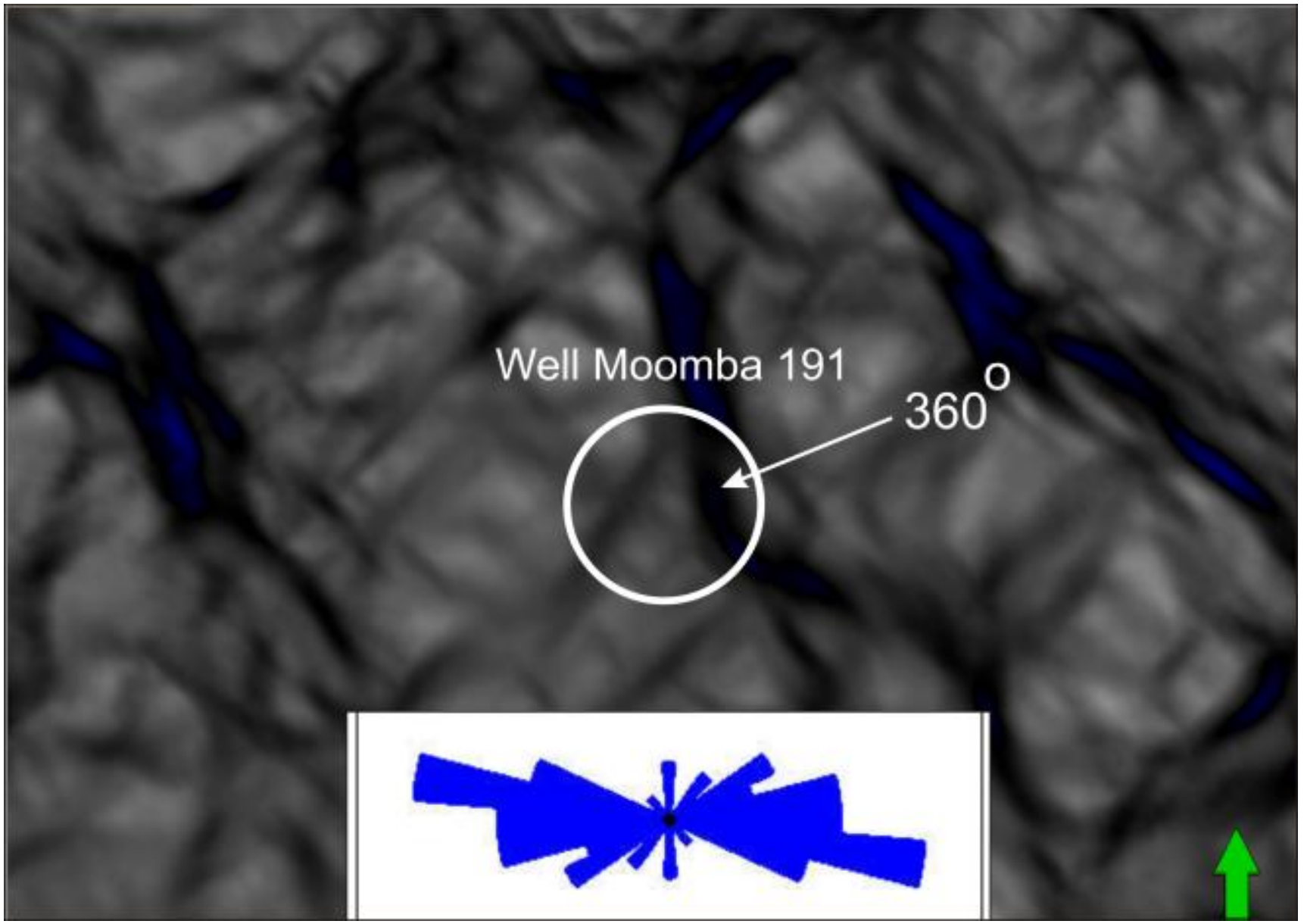

Figure 3. Most positive curvature attribute at the depth of 8776 ft showing a main signature striking north-south, and a rose diagram of image log fractures showing east-west.

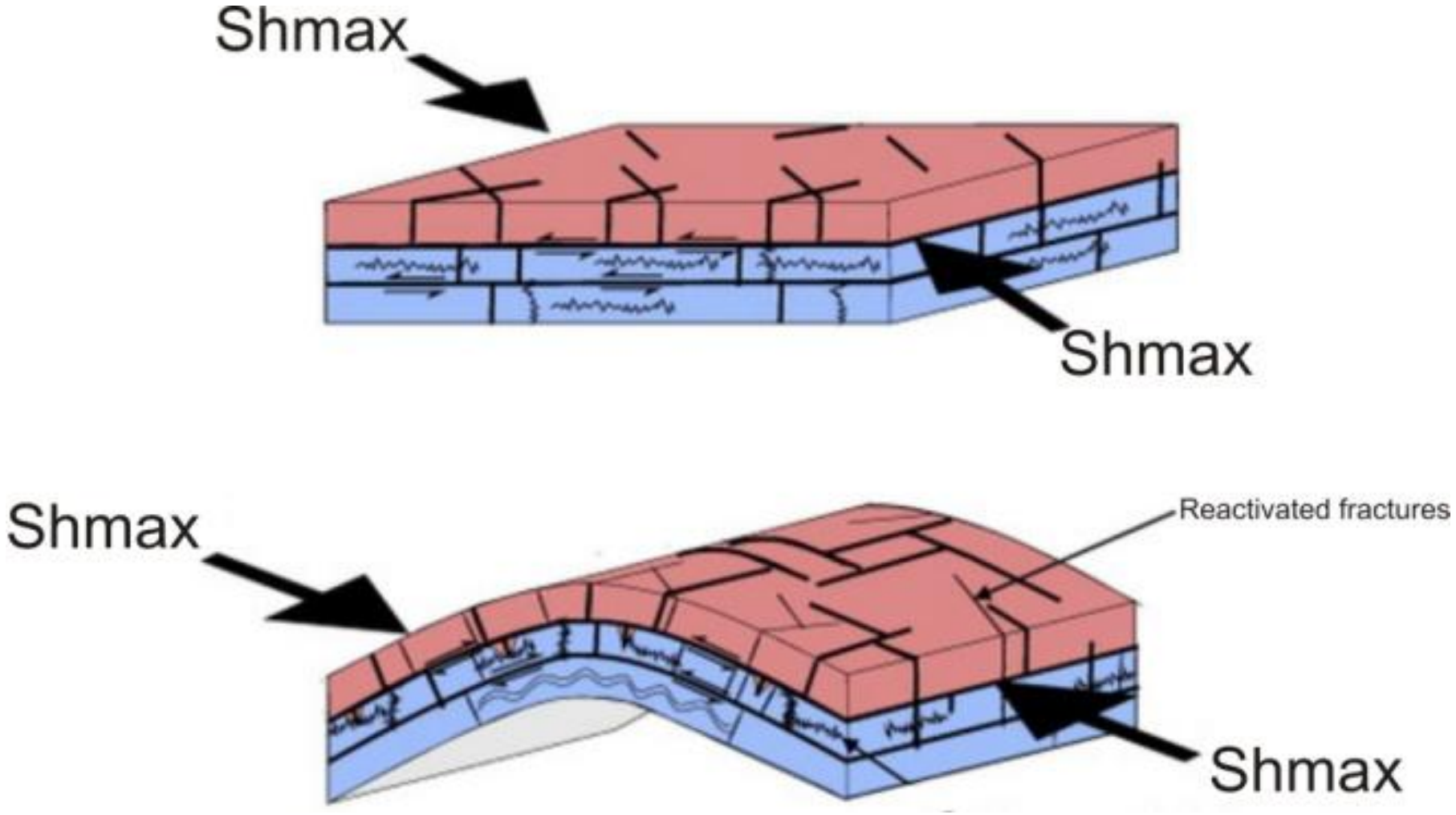

Figure 4. Schematic figure showing the generation of different sets of fractures at different tectonic stages.

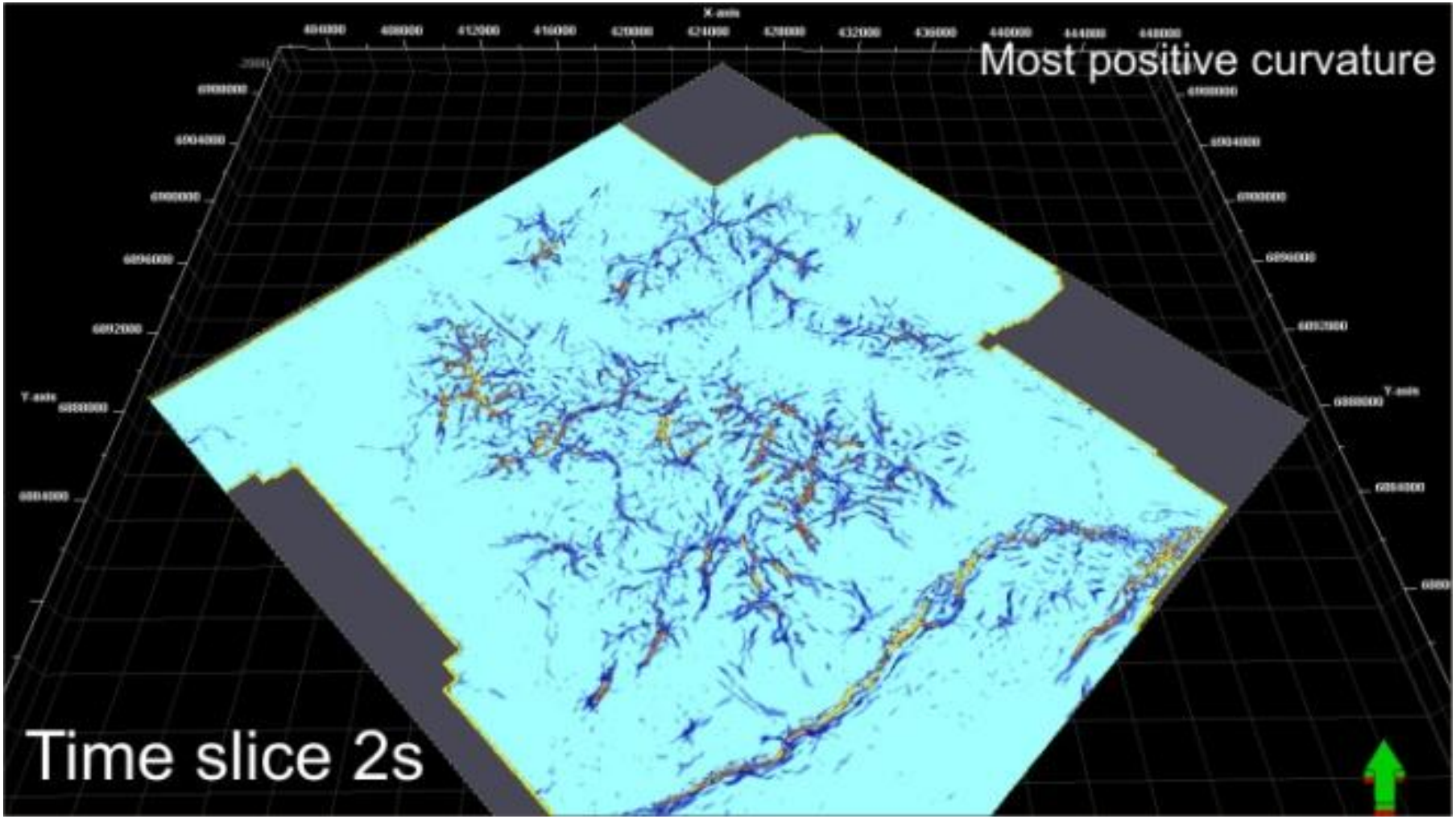

Figure 5. Most positive curvature attribute calculated after eliminating the values less or equal to 0.2, which is the cut off for Moomba field.

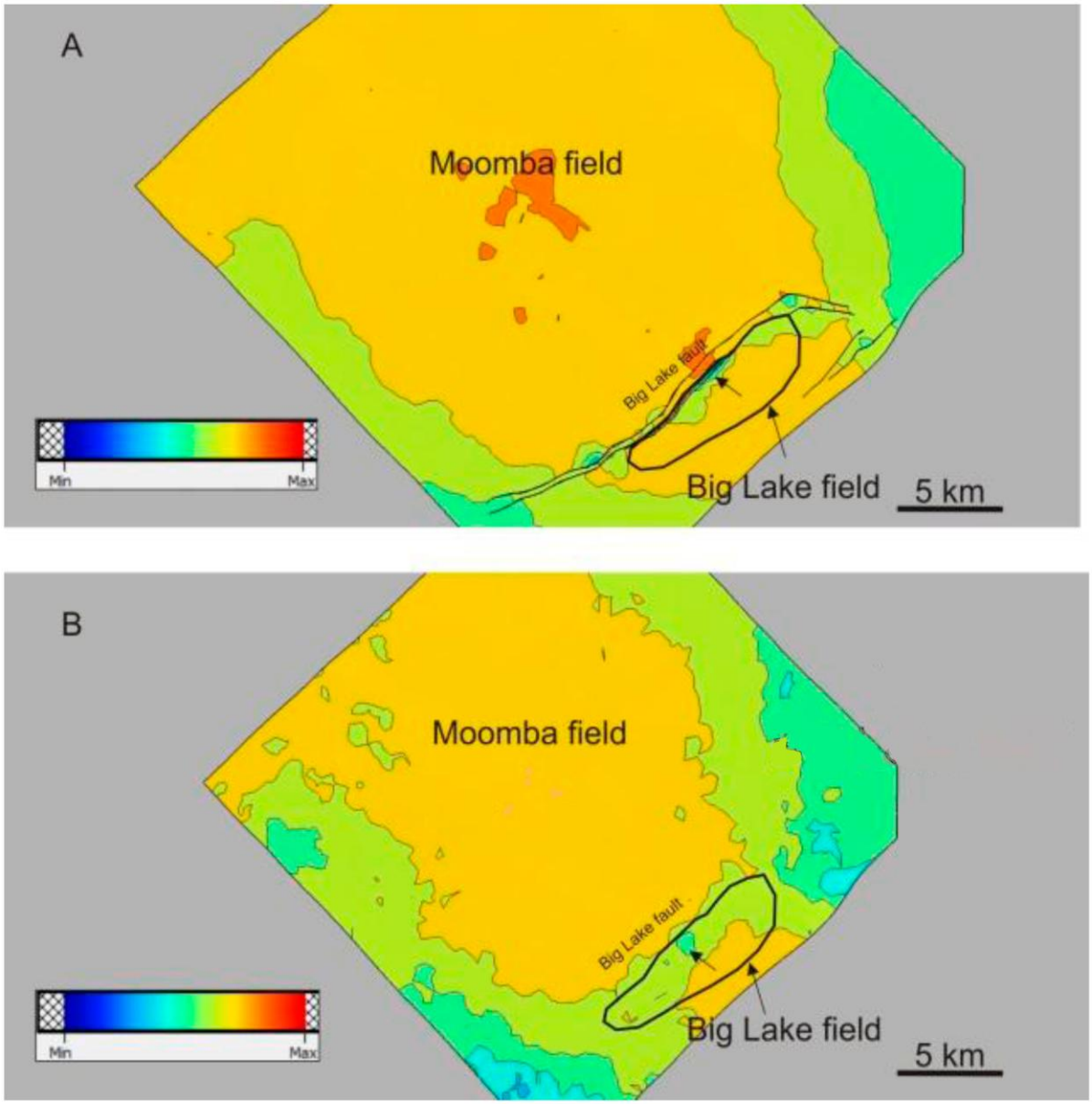

Figure 6. Map view of minimum effective stress distribution around Big Lake fault due to the effect of the paleo-stress magnitudes and orientation for: A: Patchawarra Formation, B: Toolachee Formation, using FEM. Blue colour in the Big Lake field (arrow) shows the main producing area in the field.

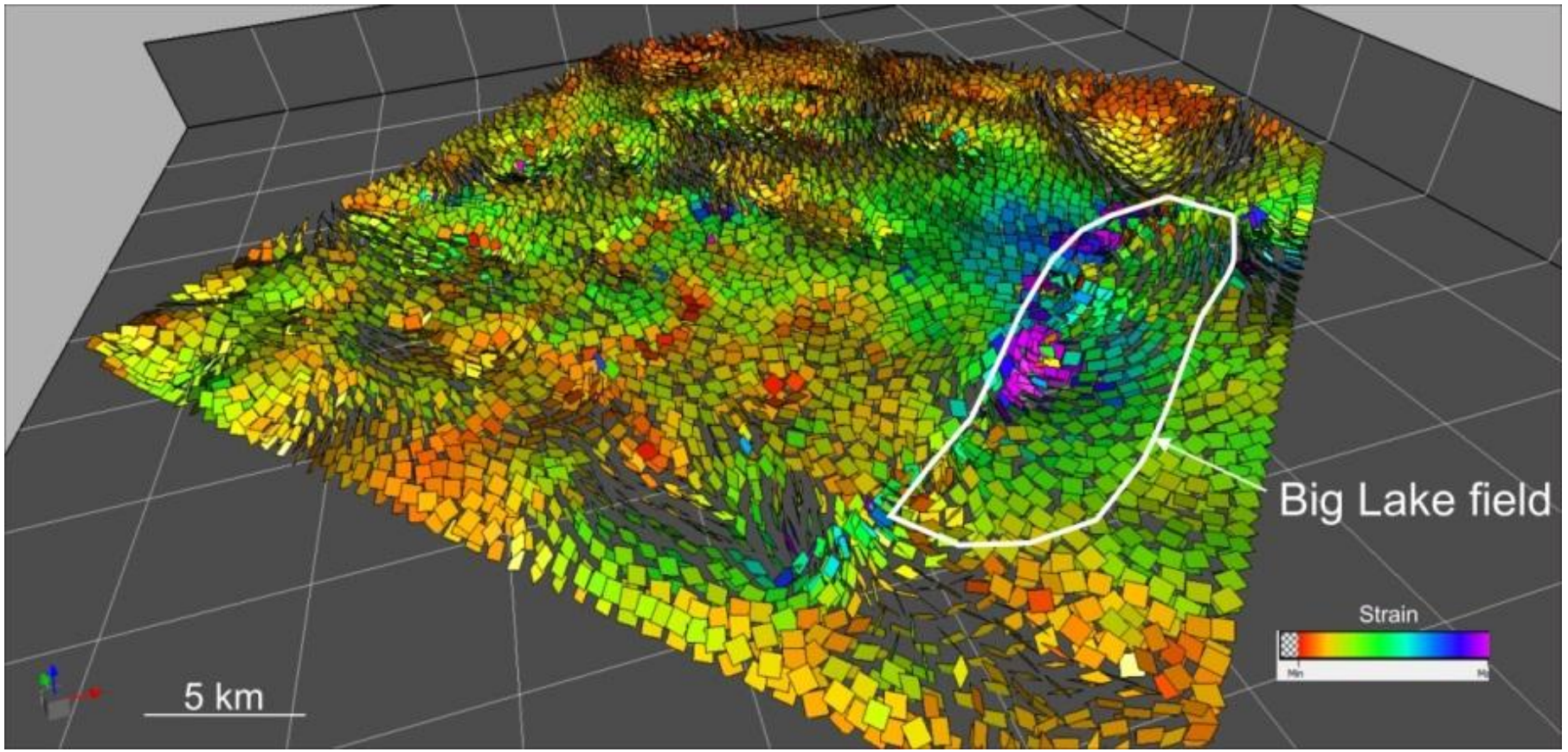

Figure 7. Predicted fracture network using stress inversion with FEM solver in *Dynel3D*. Purple colours indicate highly stressed fractures and sweet spots.

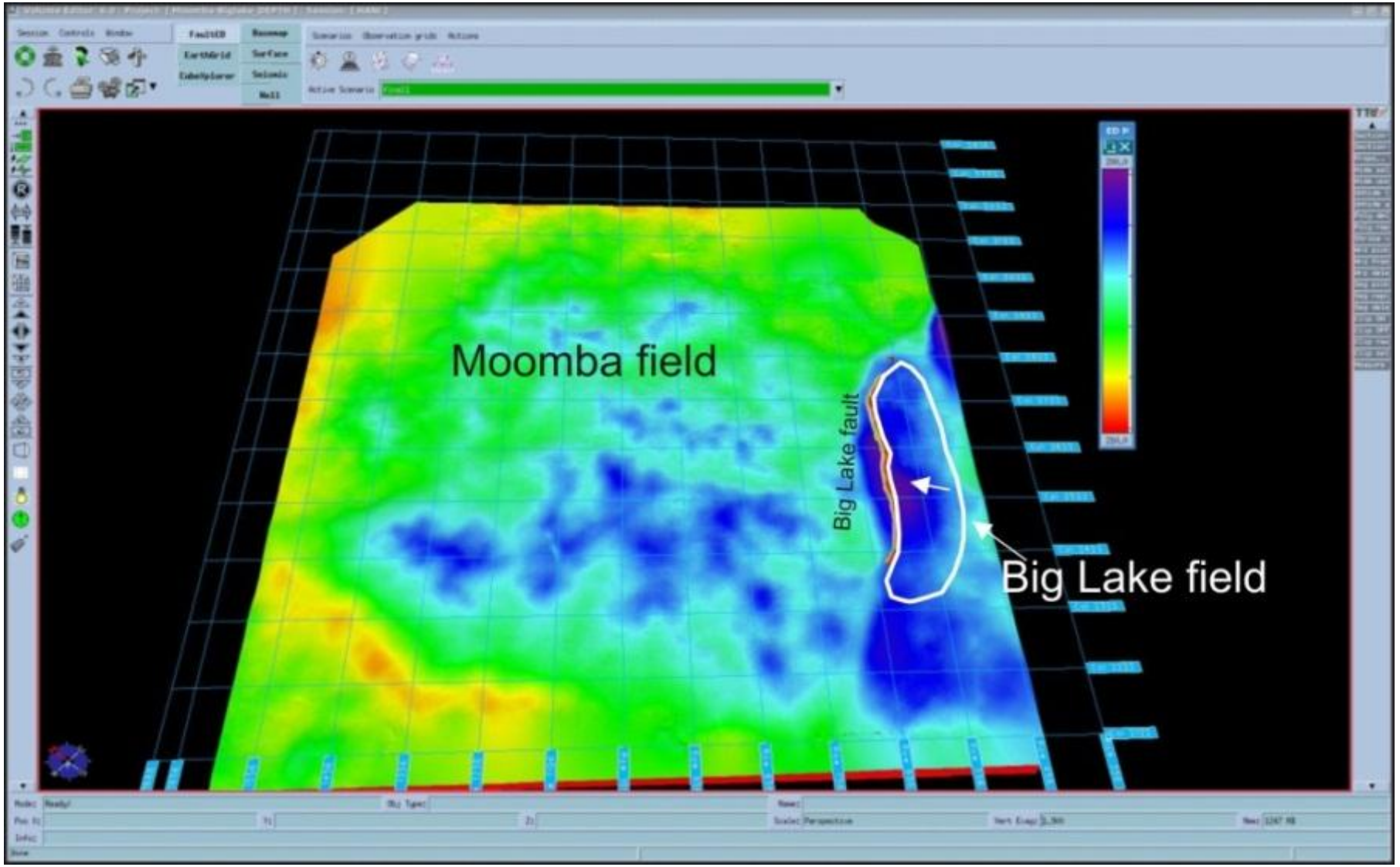

Figure 8. Map view of minimum effective stress distribution around Big Lake fault due to the effect of the paleo-stress magnitudes and orientation using BEM. Purple colour in the Big Lake field (arrow) shows the main producing area in the field.

Lithology	E (GPa)	ν	K (GPa)	G (GPa)	ρb (kg/m3)	ϕ (%)	μ (Degree)	UCS (MPa)	T (MPa)	C (MPa)
Shale	28	0.4	13	12	2530	0.63	14.4	95	3	27
Sandstone	22	0.24	14	8.87	2480	0.49	27.8	96	5	38

Table 1. Rock mechanical properties used as input data in the models.
E = Young`s modulus, ν = Poisson`s ratio, K = Bulk modulus, G = Shear modulus, ρb = Bulk Density, ϕ = Porosity, μ = Angle of friction, UCS = Unconfined Compressive strength, T = Tensile strength, C = Cohesion.